Supporting Information

Chemical Modulation of $A^{I}RE^{III}C^{IV}Q^{VI}_{4}$ Family Compounds for Band Gap and Optical Anisotropy Enhancement

Hongshan Wang,[a,b] Xueting Pan,[a], Shilie Pan[a,b*] and Junjie Li,[a,b,*]

[a]*Research Center for Crystal Materials; CAS Key Laboratory of Functional Materials and Devices for Special Environments, Xinjiang Technical Institute of Physics & Chemistry, CAS, Urumqi 830011, China*

[b]*Center of Materials Science and Optoelectronics Engineering, University of Chinese Academy of Sciences, Beijing 100049, China*

**To whom correspondence should be addressed, E-mails: slpan@ms.xjb.ac.cn (Shilie Pan), lijunjie@ms.xjb.ac.cn (Junjie Li)*

Table S1. Crystal data and structure refinements of $A^{I}RE^{III}SiQ^{VI}_4$ (A^{I} = Ag, Na; RE^{III} = La, Y; Q^{VI}= S, Se).

Empirical formula	**$AgYSiS_4$**	**$AgLaSiS_4$**	**$NaLaSiS_4$**	**$NaLaSiSe_4$**
Formula weight (Da)	353.11	403.11	318.23	505.83
Temperature (K)	298	298	221.0	298
Crystal system	Monoclinic			
Space group	$P2_1/c$			
***a*(Å)**	8.9439(19)	8.9451(8)	9.314(4)	9.8134(13)
***b*(Å)**	10.452(2)	10.5565(9)	10.470(4)	10.9219(15)
***c*(Å)**	6.5622(13)	6.9470(6)	6.868(3)	7.0956(8)
***V*(Å^3)**	588.2(2)	632.47	652.9(5)	739.82(16)
Z	4			
D_{calc} (g/cm^{-3})	3.988	4.233	3.237	4.541
Absorption coefficient (mm^{-1})	14.620	11.130	7.936	25.555
***F*(000)**	656	728	584	872
Completeness to θ (%)	98.70	100.0	100.0	98.5
θ range for data collection/°	2.375 to 27.537	2.362 to 27.492	2.243 to 27.490	3.492 to 27.491
Index ranges	-11 ≤ h ≤ 11, -13 ≤ k ≤ 13, -8 ≤ l ≤ 8	-11 ≤ h ≤ 11, -13 ≤ k ≤ 13, -8 ≤ l ≤ 9	-12 ≤ h ≤ 11, -13 ≤ k ≤ 13, -8 ≤ l ≤ 8	-12 ≤ h ≤ 11, -14 ≤ k ≤ 14, -9 ≤ l ≤ 9
Reflections collected	7287	11633	9394	5449
Independent reflections	1338 [*R*(int) = 0.0988]	1450 [*R*(int) = 0.0721]	1491 [*R*(int) = 0.0737]	1668 [*R*(int) = 0.0792]

Observed reflections [$I>2\sigma(I)$]	980	1220	1336	1400
Data / restraints / parameters	1338 / 0 / 65	1450 / 0 / 65	1491 / 0 / 65	1668 / 0 / 65
Absorpt correction type	multi-scan			
GooF on F^2	1.039	1.118	1.070	1.005
R_1, wR_2 ($I>2\sigma(I)$)[a]	0.0480, 0.1176	0.0310, 0.0750	0.0272, 0.0581	0.0404, 0.0743
R_1, wR_2 (all data)[a]	0.0713, 0.1276	0.0372, 0.0774	0.0307, 0.0607	0.0485, 0.0780
diff peak, hole (e/Å^3)	1.685, -0.971	1.456, 1.407	0.971, -0.746	1.212, 1.445

[a] $R_1=\Sigma||F_o| - |F_c||/\Sigma|F_o|$ and $wR_2 = [\Sigma w(F_o^2 - F_c^2)^2/ \Sigma wF_o^4]^{1/2}$ for $F_o^2 > 2\sigma(F_o^2)$.

Table S2. Fractional atomic coordinates, equivalent isotropic displacement parameters ($Å^2 \times 10^3$), and bond valence sum (BVS) for $AgLaSiS_4$. U_{eq} is defined as 1/3 of the trace of the orthogonalized U_{IJ} tensor.

Atoms	Wyck.	*x*	*y*	*z*	U_{eq}	BVS[a]
Ag(1)	4e	0.1122(1)	0.2458(1)	-0.0720(1)	43(1)	0.99
La(1)	4e	0.3484(1)	0.6039(1)	0.7181(1)	17(1)	2.97
Si(1)	4e	0.2573(2)	0.5499(2)	0.1903(3)	17(1)	4.08
S(1)	4e	0.4686(2)	0.6366(2)	0.3557(2)	18(1)	1.97
S(2)	4e	0.1261(2)	0.4880(2)	0.3796(2)	20(1)	1.95
S(3)	4e	0.1474(2)	0.6941(2)	-0.0111(2)	18(1)	1.99
S(4)	4e	0.3236(2)	0.4060(2)	0.0153(2)	19(1)	2.12
GII[b]						0.053

[a] The bond valence sum is calculated by bond-valence theory ($S_{ij} = \exp[(R_0-R)/B$, where R is an empirical constant, R_0 is the length of bond I (in angstroms), and B= 0.37).

[b] The global instability index (GII) calculated using

$$G = \sqrt{\frac{\sum_{i=1}^{n} (BVS - v_i)}{N}} \quad (1)$$

where N is the number of atoms in the formula unit. The GII is calculated as 0.053, which is lower than 0.2, indicating the rationality of the structure from this side.

Table S3. Fractional atomic coordinates, equivalent isotropic displacement parameters ($Å^2 \times 10^3$), and bond valence sum (BVS) for $AgYSiS_4$. U_{eq} is defined as 1/3 of the trace of the orthogonalized U_{IJ} tensor.

Atoms	**Wyck.**	***x***	***y***	***z***	**U_{eq}**	**BVS[a]**
Ag(1)	4e	0.1134(1)	0.7485(1)	-0.0667(2)	41(1)	0.94
Y(1)	4e	0.3532(1)	0.3875(1)	0.7233(1)	21(1)	2.74
Si(1)	4e	0.2644(3)	0.4484(2)	0.1985(4)	19(1)	4.14
S(1)	4e	0.4736(3)	0.3578(2)	0.3748(4)	21(1)	1.92
S(2)	4e	0.1522(3)	0.3035(2)	-0.0187(4)	21(1)	1.90
S(3)	4e	0.3308(3)	0.5886(2)	0.0066(4)	20(1)	2.06
S(4)	4e	0.1385(3)	0.5137(2)	0.4000(4)	23(1)	1.95
GII[b]						0.112

[a] The bond valence sum is calculated by bond-valence theory ($S_{ij} = \exp[(R_0-R)/B$, where R is an empirical constant, R_0 is the length of bond I (in angstroms), and B= 0.37).

[b] The global instability index (GII) calculated using

$$G = \sqrt{\frac{\sum_{i=1}^{n}(BVS - v_i)}{N}} \quad (1)$$

where N is the number of atoms in the formula unit. The GII is calculated as 0.112, which is lower than 0.2, indicating the rationality of the structure from this side.

Table S4. Fractional atomic coordinates, equivalent isotropic displacement parameters (Å^2 × 10^3), and bond valence sum (BVS) for $NaLaSiS_4$. U_{eq} is defined as 1/3 of the trace of the orthogonalized U_{IJ} tensor.

Atoms	**Wyck.**	***x***	***y***	***z***	**U_{eq}**	**BVS[a]**
Na(1)	4e	0.4116(3)	0.207(3)	0.2602(4)	53(1)	0.92
La(1)	4e	0.8579(1)	0.3946(1)	1.2317(1)	13(1)	2.91
Si(1)	4e	0.7661(1)	0.4564(1)	0.7060(2)	13(1)	4.08
S(1)	4e	0.8276(1)	0.6008(1)	0.5241(2)	15(1)	1.97
S(2)	4e	0.6599(1)	0.3115(1)	0.5104(2)	16(1)	2.06
S(3)	4e	0.6459(1)	0.5245(1)	0.9068(2)	18(1)	1.85
S(4)	4e	0.9671(1)	0.3654(1)	0.8574(2)	13(1)	2.01
GII[b]						0.073

[a] The bond valence sum is calculated by bond-valence theory (S_{ij} = exp[(R_0-R)/B, where R is an empirical constant, R_0 is the length of bond I (in angstroms), and B= 0.37).

[b] The global instability index (GII) calculated using

$$G = \sqrt{\frac{\sum_{i=1}^{n}(BVS - v_i)}{N}} \quad (1)$$

where N is the number of atoms in the formula unit. The GII is calculated as 0.073, which is lower than 0.2, indicating the rationality of the structure from this side.

Table S5. Fractional atomic coordinates, equivalent isotropic displacement parameters ($Å^2 \times 10^3$), and bond valence sum (BVS) for $NaLaSiSe_4$. U_{eq} is defined as 1/3 of the trace of the orthogonalized U_{IJ} tensor.

Atoms	**Wyck.**	***x***	***y***	***z***	**U_{eq}**	**BVS[a]**
Na(1)	4e	0.5835(7)	0.2016(6)	0.7500(8)	75(2)	0.91
La(1)	4e	0.1406(1)	0.3943(1)	-0.2323(1)	15(1)	2.76
Si(1)	4e	0.2302(3)	0.4558(2)	0.2921(3)	14(1)	4.03
Se(1)	4e	0.3372(1)	0.3085(1)	0.4967(1)	17(1)	2.03
Se(2)	4e	0.1696(1)	0.6034(1)	0.4805(1)	17(1)	1.95
Se(3)	4e	0.3571(1)	0.5239(1)	0.0907(1)	20(1)	1.78
Se(4)	4e	0.0264(1)	0.3632(1)	0.1368(1)	14(1)	1.95
GII[b]						0.116

[a] The bond valence sum is calculated by bond-valence theory ($S_{ij} = \exp[(R_0-R)/B$, where R is an empirical constant, R_0 is the length of bond I (in angstroms), and B= 0.37).

[b] The global instability index (GII) calculated using

$$G = \sqrt{\frac{\sum_{i=1}^{n}(BVS - v_i)}{N}} \quad (1)$$

where N is the number of atoms in the formula unit. The GII is calculated as 0.116, which is lower than 0.2, indicating the rationality of the structure from this side.

Table S6. Anisotropic displacement parameters ($Å^2 \times 10^3$) for $AgLaSiS_4$. The Anisotropic displacement factor exponent takes the form: $-2\pi^2[h^2a^{*2}U_{11}+2hka^*b^*U_{12}+\ldots]$.

Atoms	U_{11}	U_{22}	U_{33}	U_{23}	U_{13}	U_{12}
Ag(1)	39(1)	27(1)	65(1)	-11(1)	20(1)	-7(1)
La(1)	24(1)	15(1)	14(1)	0(1)	6(1)	2(1)
Si(1)	21(1)	14(1)	16(1)	-1(1)	6(1)	0(1)
S(1)	21(1)	14(1)	18(1)	0(1)	6(1)	-1(1)
S(2)	25(1)	19(1)	19(1)	-2(1)	10(1)	-5(1)
S(3)	22(1)	15(1)	16(1)	1(1)	3(1)	0(1)
S(4)	21(1)	16(1)	19(1)	-2(1)	6(1)	1(1)

Table S7. Anisotropic displacement parameters ($Å^2 \times 10^3$) for $AgYSiS_4$. The Anisotropic displacement factor exponent takes the form: $-2\pi^2[h^2a^{*2}U_{11}+2hka^*b^*U_{12}+\ldots]$.

Atoms	U_{11}	U_{22}	U_{33}	U_{23}	U_{13}	U_{12}
Ag(1)	45(1)	25(1)	57(1)	7(1)	17(1)	6(1)
Y(1)	29(1)	16(1)	17(1)	0(1)	7(1)	0(1)
Si(1)	28(2)	12(1)	17(1)	-1(1)	7(1)	0(1)
S(1)	27(2)	16(1)	20(1)	0(1)	9(1)	2(1)
S(2)	28(2)	16(1)	19(1)	-1(1)	6(1)	-2(1)
S(3)	28(2)	14(1)	20(1)	1(1)	8(1)	-2(1)
S(4)	32(2)	19(1)	19(1)	2(1)	11(1)	3(1)

Table S8. Anisotropic displacement parameters ($Å^2 \times 10^3$) for $NaLaSiS_4$. The Anisotropic displacement factor exponent takes the form: $-2\pi^2[h^2a^{*2}U_{11}+2hka^*b^*U_{12}+\ldots]$.

Atoms	U_{11}	U_{22}	U_{33}	U_{23}	U_{13}	U_{12}
Na(1)	58(2)	57(2)	34(1)	6(1)	-13(1)	-30(1)
La(1)	19(1)	11(1)	10(1)	0(1)	3(1)	-1(1)
Si(1)	16(1)	12(1)	10(1)	1(1)	3(1)	0(1)
S(1)	20(1)	12(1)	13(1)	2(1)	3(1)	0(1)
S(2)	19(1)	14(1)	13(1)	-1(1)	1(1)	-2(1)
S(3)	20(1)	19(1)	15(1)	1(1)	6(1)	6(1)
S(4)	16(1)	10(1)	13(1)	1(1)	3(1)	0(1)

Table S9. Anisotropic displacement parameters ($Å^2 \times 10^3$) for $NaLaSiSe_4$. The Anisotropic displacement factor exponent takes the form: $-2\pi^2[h^2a^{*2}U_{11}+2hka^*b^*U_{12}+\ldots]$.

Atoms	U_{11}	U_{22}	U_{33}	U_{23}	U_{13}	U_{12}
Na(1)	71(4)	89(5)	47(3)	-7(3)	-23(3)	49(4)
La(1)	17(1)	14(1)	13(1)	0(1)	4(1)	0(1)
Si(1)	14(1)	14(1)	14(1)	-2(1)	3(1)	0(1)
Se(1)	16(1)	19(1)	16(1)	2(1)	2(1)	2(1)
Se(2)	18(1)	16(1)	17(1)	-2(1)	3(1)	1(1)
Se(3)	20(1)	23(1)	18(1)	-1(1)	7(1)	-6(1)
Se(4)	14(1)	14(1)	15(1)	0(1)	3(1)	0(1)

Table S10. Selected bond lengths (Å) of $AgLaSiS_4$.

Atoms	Distance (Å)	Atoms	Distance (Å)
Ag(1)-S(2)#1	2.4978(19)	La(1)-S(3)#4	2.9655(16)
Ag(1)-S(3)#2	2.6149(17)	La(1)-S(4)#3	3.0270(17)
Ag(1)-S(4)	2.4897(17)	La(1)-S(4)#5	2.9866(17)
La(1)-S(1)#3	3.1361(17)	Si(1)-S(1)	2.140(2)
La(1)-S(1)#4	3.0045(17)	Si(1)-S(2)	2.086(2)
La(1)-S(1)	3.0084(16)	Si(1)-S(3)	2.124(2)
La(1)-S(2)	2.9158(17)	Si(1)-S(4)	2.126(2)
La(1)-S(3)#5	3.0779(16)		

Symmetry transformations used to generate equivalent atoms:

#1 x, -y+1/2, z-1/2; #2 -x, -y+1, -z; #3 -x+1, -y+1, -z+1; #4 x, -y+3/2, z+1/2; #5 x, y, z+1.

Table S11. Selected bond angles (°) of $AgLaSiS_4$.

Atoms	Angle (°)	Atoms	Angle (°)
S(2)#1-Ag(1)-S(3)#2	110.38(6)	S(3)#5-La(1)-S(1)#3	139.93(4)
S(4)-Ag(1)-S(2)#1	129.96(6)	S(3)#4-La(1)-S(1)	76.62(4)
S(4)-Ag(1)-S(3)#2	116.30(6)	S(3)#4-La(1)-S(3)#5	74.72(3)
S(1)#4-La(1)-S(1)	89.11(4)	S(3)#4-La(1)-S(4)#5	136.76(5)
S(1)#4-La(1)-S(1)#3	129.190(17)	S(3)#4-La(1)-S(4)#3	134.79(5)
S(1)-La(1)-S(1)#3	68.78(5)	S(4)#5-La(1)-S(1)	140.11(5)
S(1)-La(1)-S(3)#5	150.75(5)	S(4)#3-La(1)-S(1)#3	66.97(4)
S(1)#4-La(1)-S(3)#5	75.01(4)	S(4)#5-La(1)-S(1)#3	71.60(4)
S(1)#4-La(1)-S(4)#3	68.29(4)	S(4)#5-La(1)-S(1)#4	120.25(4)
S(1)-La(1)-S(4)#3	90.71(4)	S(4)#5-La(1)-S(3)#5	68.36(4)
S(2)-La(1)-S(1)#3	78.59(5)	S(4)#3-La(1)-S(3)#5	105.39(4)
S(2)-La(1)-S(1)	72.06(4)	S(4)#5-La(1)-S(4)#3	77.90(5)
S(2)-La(1)-S(1)#4	138.52(5)	S(2)-Si(1)-S(1)	111.11(10)
S(2)-La(1)-S(3)#4	71.47(5)	S(2)-Si(1)-S(3)	113.60(10)
S(2)-La(1)-S(3)#5	103.81(5)	S(2)-Si(1)-S(4)	115.21(11)
S(2)-La(1)-S(4)#5	95.97(5)	S(3)-Si(1)-S(1)	103.61(10)
S(2)-La(1)-S(4)#3	145.26(5)	S(3)-Si(1)-S(4)	106.62(10)
S(3)#4-La(1)-S(1)#3	139.70(4)	S(4)-Si(1)-S(1)	105.76(10)
S(3)#4-La(1)-S(1)#4	68.29(4)		

Symmetry transformations used to generate equivalent atoms:

#1 x, -y+1/2, z-1/2; #2 -x, -y+1, -z; #3 -x+1, -y+1, -z+1; #4 x, -y+3/2, z+1/2; #5 x, y, z+1.

Table S12. Selected bond lengths (Å) of $AgYSiS_4$.

Atoms	Distance (Å)	Atoms	Distance (Å)
Ag(1)-S(2)#3	2.647(3)	Y(1)-S(2)#5	2.850(3)
Ag(1)-S(3)	2.505(3)	Y(1)-S(3)#6	2.850(2)
Ag(1)-S(4)#1	2.511(3)	Y(1)-S(3)#4	2.889(3)
Y(1)-S(1)#4	3.235(3)	Si(1)-S(1)	2.123(4)
Y(1)-S(1)	2.808(2)	Si(1)-S(2)	2.126(4)
Y(1)-S(1)#5	2.849(3)	Si(1)-S(3)	2.124(3)
Y(1)-S(2)#6	2.932(3)	Si(1)-S(4)	2.081(3)

Symmetry transformations used to generate equivalent atoms:

#1 x, -y+3/2, z-1/2; #2 x, -y+3/2, z+1/2; #3 -x, -y+1, -z; #4 -x+1, -y+1, -z+1; #5 x, -y+1/2, z+1/2; #6 x, y, z+1.

Table S13. Selected bond angles (°) of $AgYSiS_4$.

Atoms	Angle (°)	Atoms	Angle (°)
S(3)-Ag(1)-S(2)#3	121.12(8)	S(2)#6-Y(1)-S(1)#4	140.19(7)
S(3)-Ag(1)-S(4)#1	126.39(9)	S(2)#5-Y(1)-S(2)#6	73.66(6)
S(4)#1-Ag(1)-S(2)#3	109.24(9)	S(2)#5-Y(1)-S(3)#6	136.90(8)
S(1)-Y(1)-S(1)#5	89.44(6)	S(2)#5-Y(1)-S(3)#4	139.01(8)
S(1)#5-Y(1)-S(1)#4	130.93(4)	S(3)#4-Y(1)-S(1)#4	67.09(7)
S(1)-Y(1)-S(1)#4	67.22(7)	S(3)#6-Y(1)-S(1)#4	69.49(6)
S(1)#5-Y(1)-S(2)#6	76.22(7)	S(3)#4-Y(1)-S(2)#6	108.97(7)
S(1)-Y(1)-S(2)#6	151.26(8)	S(3)#6-Y(1)-S(2)#6	71.10(7)
S(1)-Y(1)-S(2)#5	78.21(7)	S(3)#6-Y(1)-S(3)#4	76.94(8)
S(1)#5-Y(1)-S(2)#5	71.32(8)	S(1)-Si(1)-S(2)	102.86(14)
S(1)#5-Y(1)-S(3)#4	69.92(7)	S(1)-Si(1)-S(3)	106.23(16)
S(1)-Y(1)-S(3)#4	88.54(8)	S(3)-Si(1)-S(2)	104.62(14)
S(1)-Y(1)-S(3)#6	136.64(7)	S(4)-Si(1)-S(1)	110.60(14)
S(1)#5-Y(1)-S(3)#6	121.71(7)	S(4)-Si(1)-S(2)	114.97(17)
S(2)#5-Y(1)-S(1)#4	136.68(7)	S(4)-Si(1)-S(3)	116.34(14)

Symmetry transformations used to generate equivalent atoms:

#1 x, -y+3/2, z-1/2; #2 x, -y+3/2, z+1/2; #3 -x, -y+1, -z; #4 -x+1, -y+1, -z+1; #5 x, -y+1/2, z+1/2; #6 x, y, z+1.

Table S14. Selected bond lengths (Å) of $NaLaSiS_4$.

Atoms	Distance (Å)	Atoms	Distance (Å)
Na(1)-S(1)#4	2.841(3)	La(1)-S(2)#6	3.0647(15)
Na(1)-S(2)#1	3.178(4)	La(1)-S(3)	2.9601(14)
Na(1)-S(2)	2.780(3)	La(1)-S(4)	2.9837(15)
Na(1)-S(3)#5	3.039(3)	La(1)-S(4)#2	2.9668(15)
Na(1)-S(3)#3	3.116(3)	La(1)-S(4)#7	3.1288(15)
Na(1)-S(3)#1	3.267(4)	Si(1)-S(1)	2.1194(17)
La(1)-S(1)#6	3.0041(14)	Si(1)-S(2)	2.1203(17)
La(1)-S(1)#7	3.0348(17)	Si(1)-S(3)	2.0861(18)
La(1)-S(2)#2	3.0199(14)	Si(1)-S(4)	2.1515(18)

Symmetry transformations used to generate equivalent atoms:

#1 x, -y+1/2, z-1/2; #2 x, -y+1/2, z+1/2; #3 -x+1, y-1/2, -z+3/2; #4 -x+1, y-1/2, -z+1/2; #5 -x+1, -y+1, -z+1; #6 x, y, z+1; #7 -x+2, -y+1, b-z+2.

Table S15. Selected bond angles (°) of $NaLaSiS_4$.

Atoms	Angle (°)	Atoms	Angle (°)
S(1)#4-Na(1)-S(2)#1	99.12(9)	S(3)-La(1)-S(1)#6	91.59(4)
S(1)#4-Na(1)-S(3)#3	91.60(8)	S(3)-La(1)-S(1)#7	144.01(4)
S(1)#4-Na(1)-S(3)#1	106.81(10)	S(3)-La(1)-S(2)#6	102.01(4)
S(1)#4-Na(1)-S(3)#5	93.29(9)	S(3)-La(1)-S(2)#2	73.67(4)
S(2)-Na(1)-S(1)#4	174.68(13)	S(3)-La(1)-S(4)	72.30(4)
S(2)-Na(1)-S(2)#1	75.65(8)	S(3)-La(1)-S(4)#2	140.24(3)
S(2)-Na(1)-S(3)#5	85.50(8)	S(3)-La(1)-S(4)#7	76.88(4)
S(2)#1-Na(1)-S(3)#1	66.72(8)	S(4)-La(1)-S(1)#6	138.64(3)
S(2)-Na(1)-S(3)#1	72.22(8)	S(4)#2-La(1)-S(1)#7	68.11(3)
S(2)-Na(1)-S(3)#3	92.47(8)	S(4)#2-La(1)-S(1)#6	122.82(4)
S(3)#5-Na(1)-S(2)#1	86.59(8)	S(4)-La(1)-S(1)#7	90.31(4)
S(3)#3-Na(1)-S(2)#1	128.56(12)	S(4)-La(1)-S(2)#6	151.27(3)
S(3)#5-Na(1)-S(3)#1	148.45(10)	S(4)#2-La(1)-S(2)#2	67.79(4)
S(3)#3-Na(1)-S(3)#1	62.02(7)	S(4)-La(1)-S(2)#2	77.30(4)
S(3)#5-Na(1)-S(3)#3	143.12(13)	S(4)#2-La(1)-S(2)#6	76.86(4)
S(1)#6-La(1)-S(1)#7	80.91(4)	S(4)#2-La(1)-S(4)#7	129.35(3)
S(1)#7-La(1)-S(2)#6	107.47(4)	S(4)-La(1)-S(4)#7	67.76(4)
S(1)#6-La(1)-S(2)#2	135.43(4)	S(4)#2-La(1)-S(4)	89.76(3)
S(1)#6-La(1)-S(2)#6	68.14(4)	S(1)-Si(1)-S(2)	106.63(7)
S(1)#7-La(1)-S(4)#7	67.33(4)	S(1)-Si(1)-S(4)	106.30(8)
S(1)#6-La(1)-S(4)#7	71.59(4)	S(2)-Si(1)-S(4)	102.82(7)
S(2)#2-La(1)-S(1)#7	134.07(3)	S(3)-Si(1)-S(1)	113.67(8)
S(2)#2-La(1)-S(2)#6	74.13(3)	S(3)-Si(1)-S(2)	114.85(8)
S(2)#6-La(1)-S(4)#7	139.67(3)	S(3)-Si(1)-S(4)	111.67(7)
S(2)#2-La(1)-S(4)#7	139.63(4)		

Symmetry transformations used to generate equivalent atoms:

#1 x, -y+1/2, z-1/2; #2 x, -y+1/2, z+1/2; #3 -x+1, y-1/2, -z+3/2; #4 -x+1, y-1/2, -z+1/2; #5 -x+1, -y+1, -z+1; #6 x, y, z+1; #7 -x+2, -y+1, b-z+2.

Table S16. Selected bond lengths (Å) of $NaLaSiSe_4$.

Atoms	Distance (Å)	Atoms	Distance (Å)
Na(1)-Se(1)#1	3.298(7)	La(1)-Se(2)#7	3.1440(11)
Na(1)-Se(1)	2.902(5)	La(1)-Se(3)	3.0843(11)
Na(1)-Se(2)#3	2.921(5)	La(1)-Se(4)#2	3.0899(10)
Na(1)-Se(3)#4	3.210(6)	La(1)-Se(4)	3.0969(11)
Na(1)-Se(3)#5	3.256(6)	La(1)-Se(4)#7	3.2670(11)
Na(1)-Se(3)#1	3.334(7)	Si(1)-Se(1)	2.257(3)
La(1)-Se(1)#6	3.1654(11)	Si(1)-Se(2)	2.260(3)
La(1)-Se(1)#2	3.1332(11)	Si(1)-Se(3)	2.229(3)
La(1)-Se(2)#6	3.1166(11)	Si(1)-Se(4)	2.284(3)

Symmetry transformations used to generate equivalent atoms:

#1 x, -y+1/2, z+1/2; #2 x, -y+1/2, z-1/2; #3 -x+1, y-1/2, -z+3/2; #4 -x+1, -y+1, -z+1; #5 -x+1, y-1/2, -z+1/2; #6 x, y, z-1; #7 -x, -y+1, -z.

Table S17. Selected bond angles (°) of $NaLaSiSe_4$.

Atoms	Angle (°)	Atoms	Angle (°)
Se(1)-Na(1)-Se(1)#1	74.61(15)	Se(3)-La(1)-Se(1)#2	72.75(3)
Se(1)-Na(1)-Se(2)#3	177.1(2)	Se(3)-La(1)-Se(1)#6	100.10(3)
Se(1)-Na(1)-Se(3)#4	84.22(14)	Se(3)-La(1)-Se(2)#7	145.43(3)
Se(1)-Na(1)-Se(3)#5	92.66(14)	Se(3)-La(1)-Se(2)#6	89.90(3)
Se(1)-Na(1)-Se(3)#1	72.13(14)	Se(3)-La(1)-Se(4)#2	141.30(3)
Se(1)#1-Na(1)-Se(3)#1	69.06(15)	Se(3)-La(1)-Se(4)#7	76.49(3)
Se(2)#3-Na(1)-Se(1)#1	103.84(18)	Se(3)-La(1)-Se(4)	75.16(3)
Se(2)#3-Na(1)-Se(3)#1	109.72(19)	Se(4)#2-La(1)-Se(1)#2	69.47(3)
Se(2)#3-Na(1)-Se(3)#4	93.29(16)	Se(4)-La(1)-Se(1)#2	77.52(3)
Se(2)#3-Na(1)-Se(3)#5	90.18(15)	Se(4)-La(1)-Se(1)#6	150.72(3)
Se(3)#4-Na(1)-Se(1)#1	86.55(14)	Se(4)#2-La(1)-Se(1)#6	77.15(3)
Se(3)#5-Na(1)-Se(1)#1	130.8(2)	Se(4)#2-La(1)-Se(2)#7	66.57(3)
Se(3)#4-Na(1)-Se(3)#1	149.5(2)	Se(4)-La(1)-Se(2)#6	137.64(3)
Se(3)#5-Na(1)-Se(3)#1	61.83(11)	Se(4)-La(1)-Se(2)#7	88.95(3)
Se(3)#4-Na(1)-Se(3)#5	140.3(3)	Se(4)#2-La(1)-Se(2)#6	123.50(3)
Se(1)#2-La(1)-Se(1)#6	73.55(2)	Se(4)-La(1)-Se(4)#7	67.44(3)
Se(1)#2-La(1)-Se(2)#7	134.13(3)	Se(4)#2-La(1)-Se(4)	88.69(3)
Se(1)#2-La(1)-Se(4)#7	138.06(3)	Se(4)#2-La(1)-Se(4)#7	129.48(2)
Se(1)#6-La(1)-Se(4)#7	140.51(3)	Se(1)-Si(1)-Se(2)	105.95(10)
Se(2)#7-La(1)-Se(1)#6	108.02(3)	Se(1)-Si(1)-Se(4)	102.68(10)
Se(2)#6-La(1)-Se(1)#2	135.92(3)	Se(2)-Si(1)-Se(4)	106.25(11)
Se(2)#6-La(1)-Se(1)#6	70.06(3)	Se(3)-Si(1)-Se(1)	113.86(12)
Se(2)#6-La(1)-Se(2)#7	81.42(3)	Se(3)-Si(1)-Se(2)	113.85(11)
Se(2)#6-La(1)-Se(4)#7	70.60(3)	Se(3)-Si(1)-Se(4)	113.29(10)
Se(2)#7-La(1)-Se(4)#7	69.05(3)		

Symmetry transformations used to generate equivalent atoms:

#1 x, -y+1/2, z+1/2; #2 x, -y+1/2, z-1/2; #3 -x+1, y-1/2, -z+3/2; #4 -x+1, -y+1, -z+1; #5 -x+1, y-1/2, -z+1/2; #6 x, y, z-1; #7 -x, -y+1, -z.

Table S18. Structure and optical properties of the $A^{I}RE^{III}C^{IV}Q^{VI}_4$ (A^{I} = Ag, Li ~ Cs; RE^{III} = Y, La ~ Nd, Sm ~ Yb; C^{IV} = Si, Ge; Q^{VI} = S, Se) family compounds.

No.	Compound	Space group	Band gap (eV)	SHG(× AGS)	LIDT(×AGS)	Δ*n*	Ref
1	$AgLaSiS_4$	$P2_1/c$	3.33[a]	/	/	0.114	*c*
2	$AgYSiS_4$	$P2_1/c$	3.18[a]	/	/	0.129	*c*
3	$NaLaSiS_4$	$P2_1/c$	3.83[b]	/	/	0.130	*c*
4	$NaLaSiSe_4$	$P2_1/c$	3.02[b]	/	/	0.160	*c*
5	$LiLaSiS_4$	*Ama*2	3.71[a]	2	14	0.033	1
6	$LiCeSiS_4$	*Ama*2	2.92[a]	2.1	9	0.054	1
7	$KLaSiS_4$	$P2_1$	3.31[b]	0.2	/	0.048	2
8	$KLaSiS_4$	$P2_1/m$	/	/	/	/	3
9	$KYSiS_4$	$P2_1$	3.58[b]	0.3	/	0.080	2
10	$KCeSiS_4$	$P2_1$	2.33-2.51[a]	/	/	/	4
11	$KCeSiS_4$	$P2_1/m$	/	/	/	/	5
12	$KPrSiS_4$	$P2_1$	/	/	/	/	6
13	$KNdSiS_4$	$P2_1$	/	/	/	/	6
14	$KEuSiS_4$	$P2_1$	1.72[a]	/	/	/	7
15	$KYbSiS_4$	$P2_1$	/	/	/	/	8
16	$KLaSiSe_4$	$P2_1$	2.76[b]	0.5	/	0.080	2
17	$KPrSiSe_4$	$P2_1$	/	/	/	/	9
18	$KLaGeS_4$	$P2_1$	3.34[a]	1.2	/	0.098	10
19	$KYGeS_4$	$P2_1$	3.15[a]	1	/	0.12	11
20	$KNdGeS_4$	$P2_1$	/	/	/	/	12
21	$KEuGeS_4$	$P2_1$	1.71[a]	/	/	/	7
22	$KGdGeS_4$	$P2_1$	/	/	/	/	12
23	$KTbGeS_4$	$P2_1$	/	/	/	/	13
24	$KLaGeSe_4$	$P2_1$	2.47[b]	1.2	/	0.106	2
25	$KCeGeSe_4$	$P2_1$	1.70-1.93[a]	/	/	/	9
26	$KPrGeSe_4$	$P2_1$	/	/	/	/	13
27	$KSmGeSe_4$	$P2_1$	2.2[a]	/	/	/	14
28	$RbLaSiS_4$	*Pnma*	/	/	/	/	3
29	$RbCeSiS_4$	*Pnma*	/	/	/	/	6

30	$RbPrSiS_4$	$P2_12_12_1$	/	/	/	/	6
31	$RbNdSiS_4$	$P2_12_12_1$	/	/	/	/	6
32	$RbEuSiS_4$	$P2_12_12_1$	/	/	/	/	15
33	$RbGdSiS_4$	$P2_12_12_1$	/	/	/	/	6
34	$RbTbSiS_4$	$P2_12_12_1$	/	/	/	/	6
35	$RbDySiS_4$	$P2_12_12_1$	/	/	/	/	6
36	$RbHoSiS_4$	$P2_12_12_1$	/	/	/	/	6
37	$RbLaGeS_4$	$P2_12_12_1$	/	/	/	/	6
38	$RbEuGeS_4$	$P2_1/m$	/	/	/	/	9
39	$RbSmGeSe_4$	$P2_12_12_1$	2.2[a]	/	/	/	14
40	$CsLaSiS_4$	*Pnma*	/	/	/	/	6
41	$CsCeSiS_4$	*Pnma*	/	/	/	/	16
42	$CsPrSiS_4$	$P2_12_12_1$	/	/	/	/	6
43	$CsNdSiS_4$	$P2_12_12_1$	/	/	/	/	6
44	$CsSmSiS_4$	$P2_12_12_1$	/	/	/	/	17
45	$CsEuSiS_4$	$P2_12_12_1$	/	/	/	/	17
46	$CsGdSiS_4$	$P2_12_12_1$	/	/	/	/	17
47	$CsTbSiS_4$	$P2_12_12_1$	/	/	/	/	17
48	$CsDySiS_4$	$P2_12_12_1$	/	/	/	/	17
49	$CsHoSiS_4$	$P2_12_12_1$	/	/	/	/	17
50	$CsErSiS_4$	$P2_12_12_1$	/	/	/	/	17
51	$CsTmSiS_4$	$P2_12_12_1$	/	/	/	/	17
52	$CsCeSiSe_4$	$P2_12_12_1$	/	/	/	/	16
53	$CsLaGeS_4$	$P2_12_12_1$	3.6[a]	0.01	/	/	6
54	$CsCeGeS_4$	$P2_12_12_1$	/	/	/	/	6
55	$CsPrGeS_4$	$P2_12_12_1$	/	/	/	/	6
56	$CsNdGeS_4$	$P2_12_12_1$	/	/	/	/	6
57	$CsSmGeS_4$	$P2_12_12_1$	/	/	/	/	18
58	$CsEuGeS_4$	$P2_12_12_1$	/	/	/	/	6
59	$CsGdGeS_4$	$P2_1/n$	/	/	/	/	6
60	$CsTbGeS_4$	$P2_12_12_1$	/	/	/	/	6
61	$CsSmGeSe_4$	$P2_12_12_1$	2.2[a]	/	/	/	14

a: experimental band gap; *b*: theoretical band gap; *c*: this work.

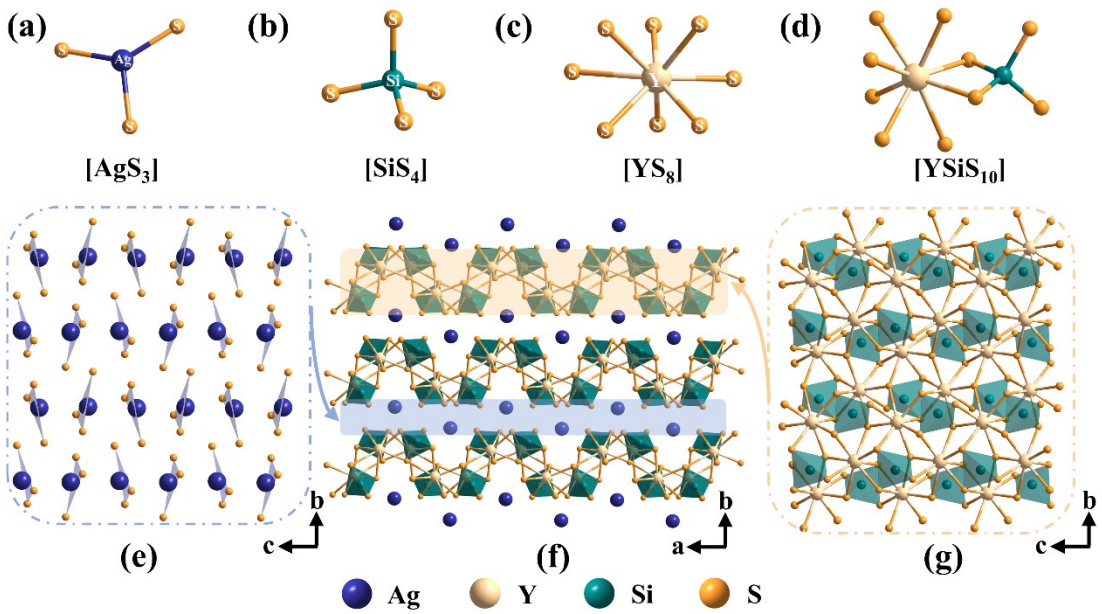

Figure S1. Crystal structure of $AgYSiS_4$. (a, b, c) The coordination environments of Ag, Si, and Y atoms in the compound; (d) The formed $[YSiS_{10}]$ dimer; (e) The formed $[AgS_3]$ pseudo-layers in $AgYSiS_4$; (f) The 3D crystal structure of $AgYSiS_4$ viewed along *c* direction; (g) The formed 2D $[YSiS_{10}]_\infty$ layers viewed along *a* direction.

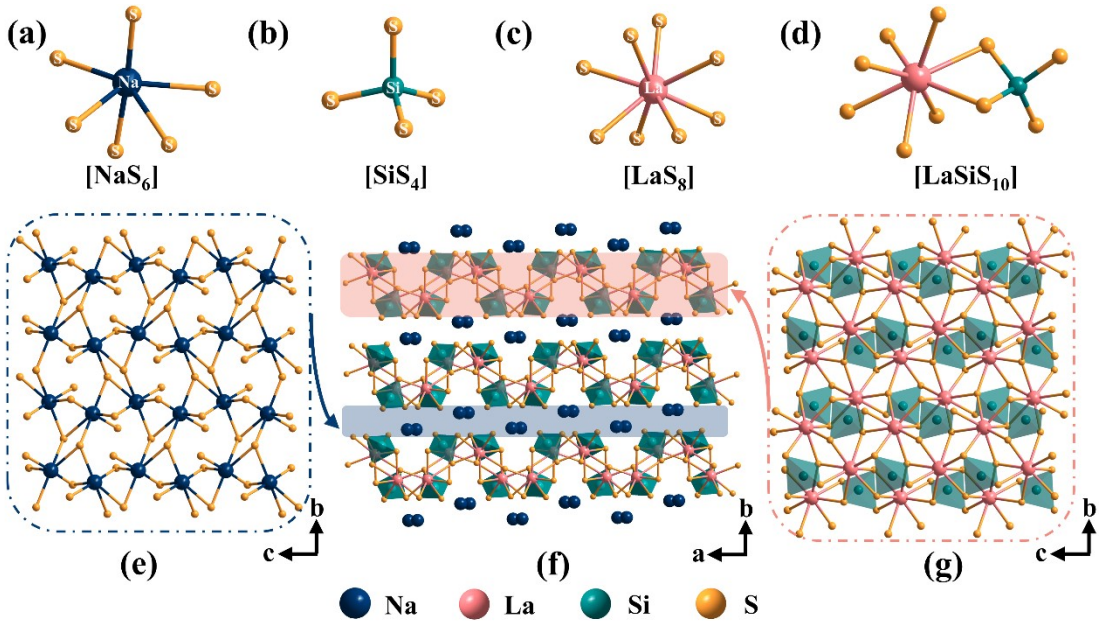

Figure S2. Crystal structure of $NaLaSiS_4$. (a-c) The coordination environments of Na, Si, and La atoms in the compound; (d) The formed $[LaSiS_{10}]$ dimer; (e) The formed channel-like $[NaS_6]_\infty$ framework in $NaLaSiS_4$; (f) The 3D crystal structure of $NaLaSiS_4$ viewed along *c* direction; (g) The formed 2D $[LaSiS_{10}]_\infty$ layers viewed along *a* direction.

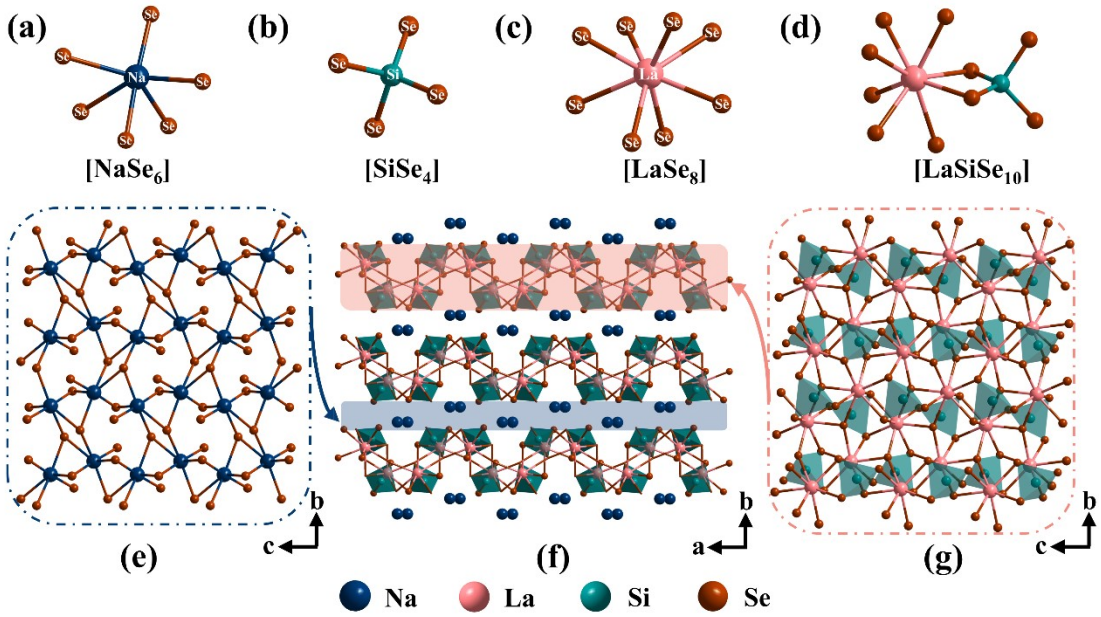

Figure S3. Crystal structure of $NaLaSiSe_4$. (a-c) The coordination environments of Na, Si, and La atoms in the compound; (d) The formed $[LaSiSe_{10}]$ dimer; (e) The formed channel-like $[NaSe_6]_\infty$ framework in $NaLaSiSe_4$; (f) The 3D crystal structure of $NaLaSiSe_4$ viewed along *c* direction; (g) The formed 2D $[LaSiSe_{10}]_\infty$ layers viewed along *a* direction.

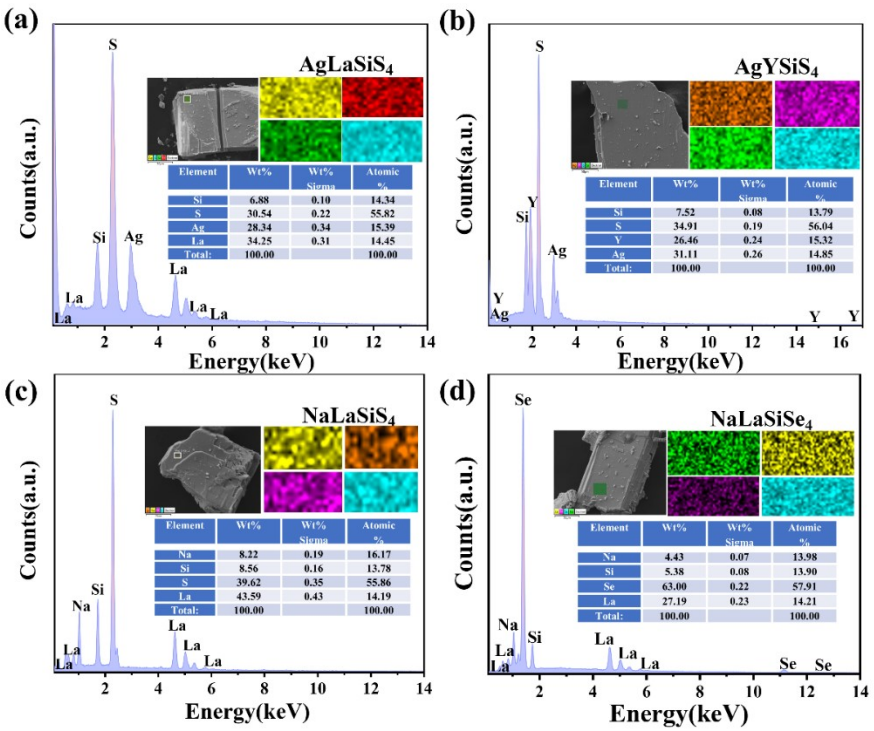

Figure S4. X-ray energy dispersive spectra and mappings of (a) $AgLaSiS_4$, (b) $AgYSiS_4$, (c) $NaLaSiS_4$, and (d) $NaLaSiSe_4$.

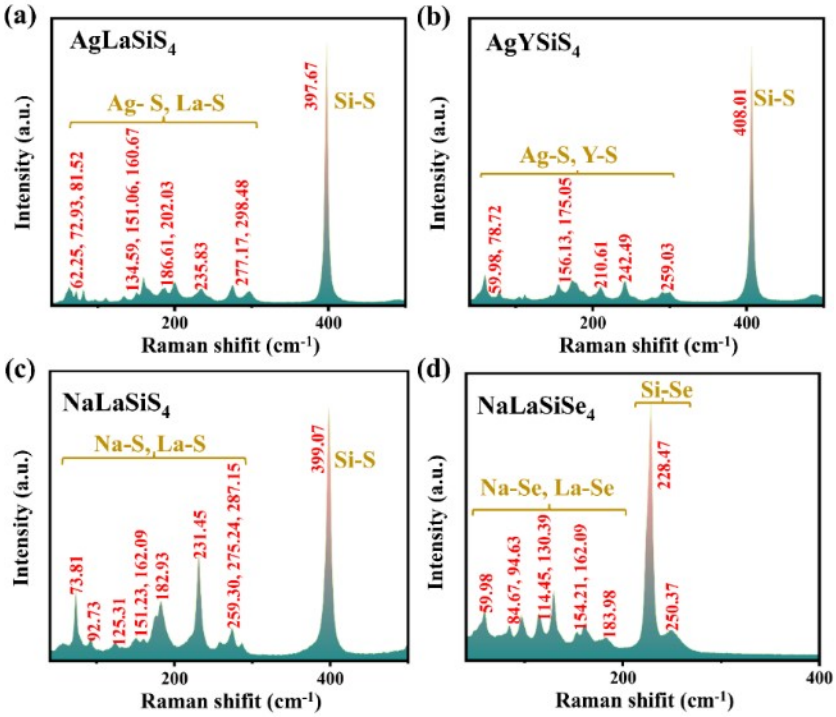

Figure S5. Raman spectra of (a) $AgLaSiS_4$, (b) $AgYSiS_4$, (c) $NaLaSiS_4$, and (d) $NaLaSiSe_4$.

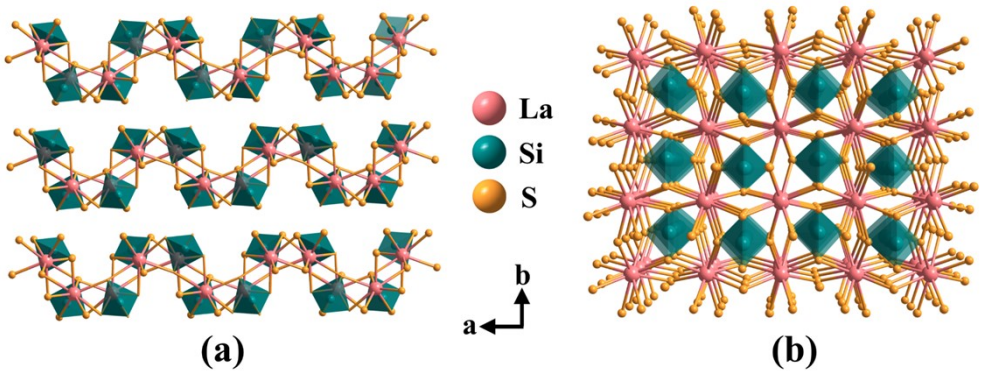

Figure S6. The $[LaSiS]_{\infty}$ framework shape built by $[LaS_8]$ and $[SiS_4]$ in (a) $ALaSiS_4$ (A = Ag, Na, K, Rb, Cs), (b) $LiLaSiS_4$.

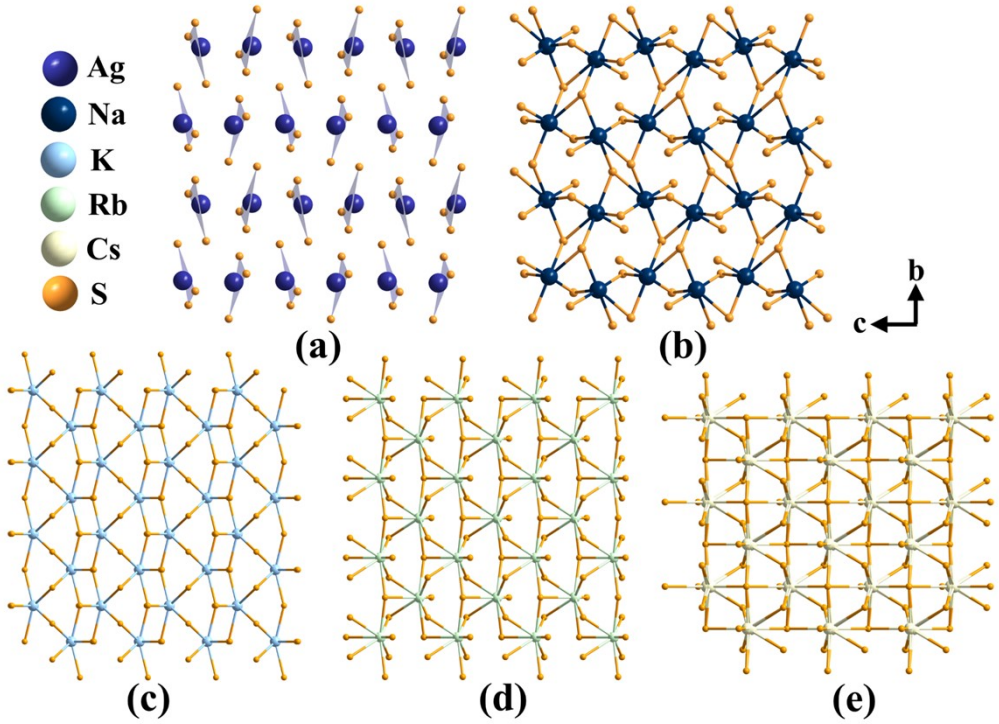

Figure S7. The $[AgS_3]$ (a), $[NaS_6]$ (b), $[KS_8]$ (c), $[RbS_8]$ (d), and $[CsS_8]$ (d) framework in $ALaSiS_4$ (A = Ag, Na, K, Rb, Cs).

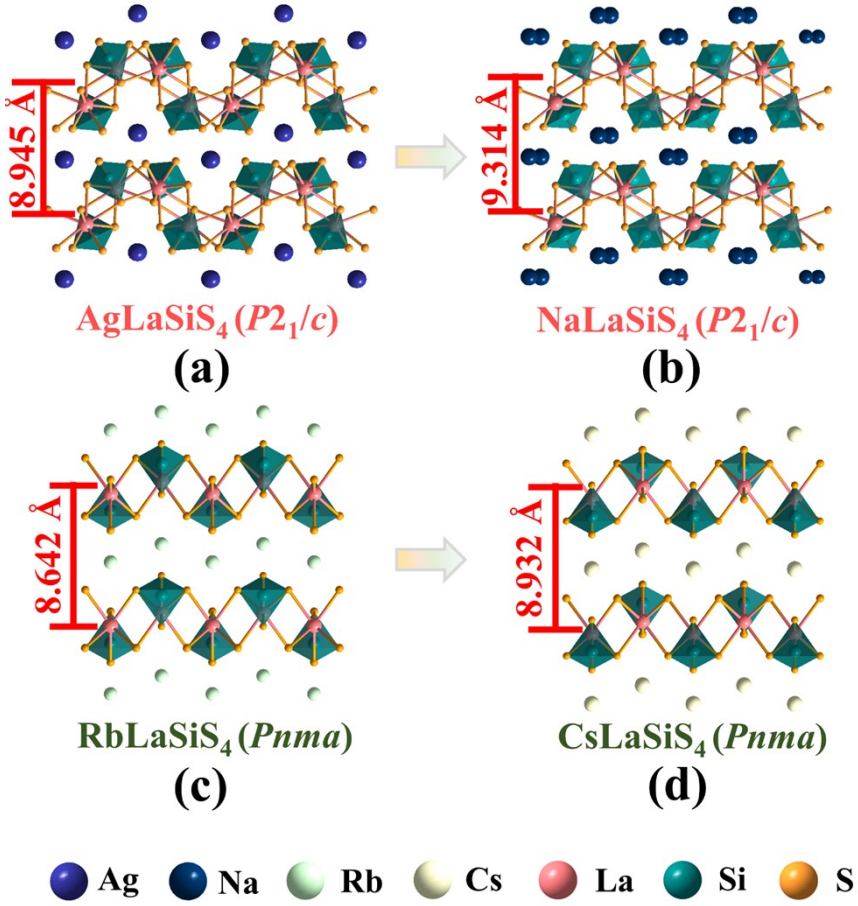

Figure S8. The variation of layer spacing from $AgLaSiS_4$ to $NaLaSiS_4$ (a-b), and from $RbLaSiS_4$ to $CsLaSiS_4$ (c-d).

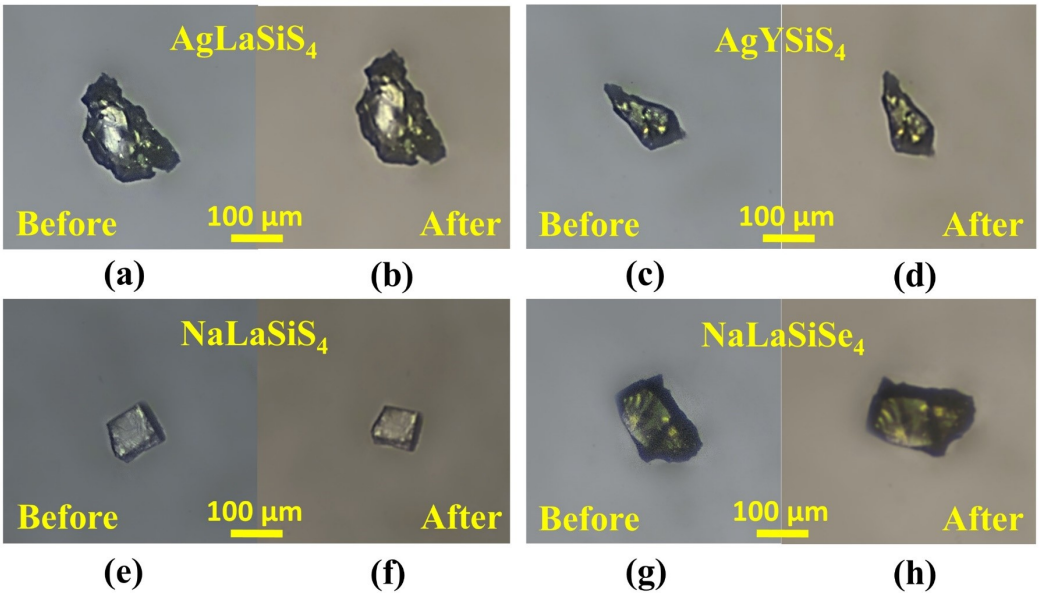

Figure S9. The optical images of $A^{I}RE^{III}SiQ^{VI}_4$ (A^{I} = Ag, Na; RE^{III} = La, Y; Q^{VI} = S, Se) before (a, c, e, g) and after (b, d, f, h) soaking in deionized water for 7 days.

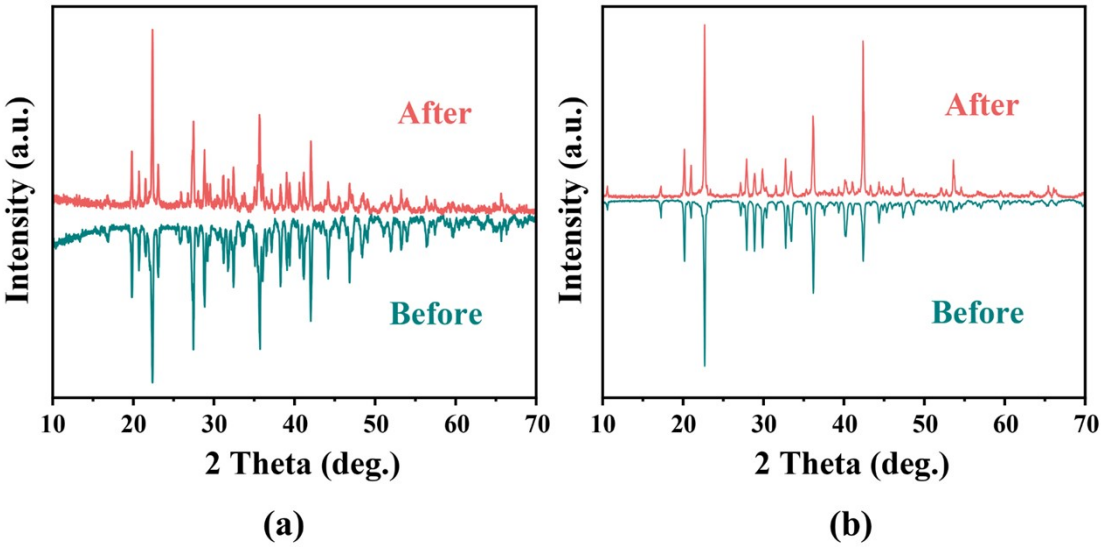

Figure S10. The XRD patterns of the polycrystalline $AgLaSiS_4$ (a) and $AgYSiS_4$ (b) powder samples before and after exposure in air for 6 months.

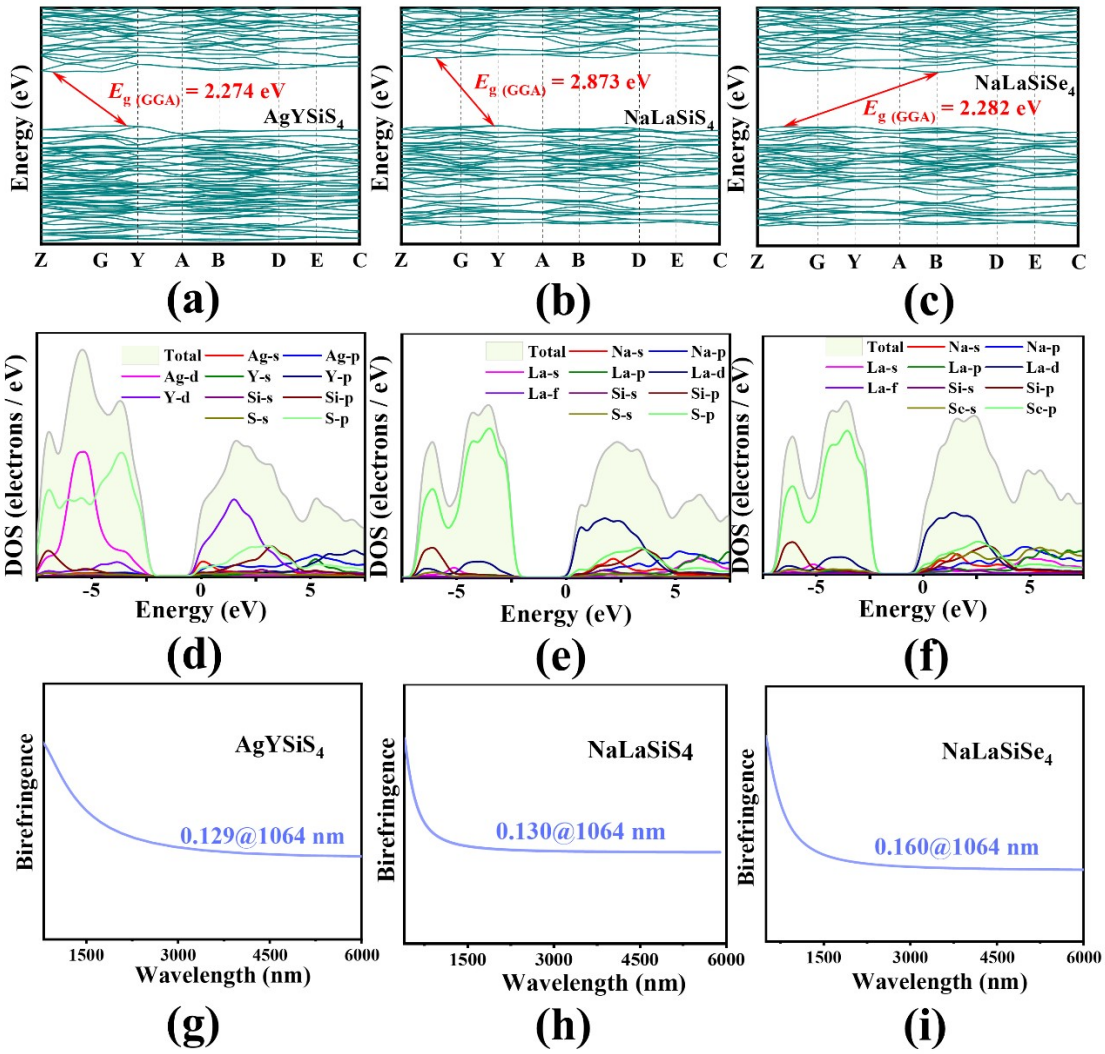

Figure S11. The band structures, the total and partial density of states and the birefringence curves of (a, d, g) $AgYSiS_4$, (b, e, h) $NaLaSiS_4$, and (c, f, i) $NaLaSiSe_4$.

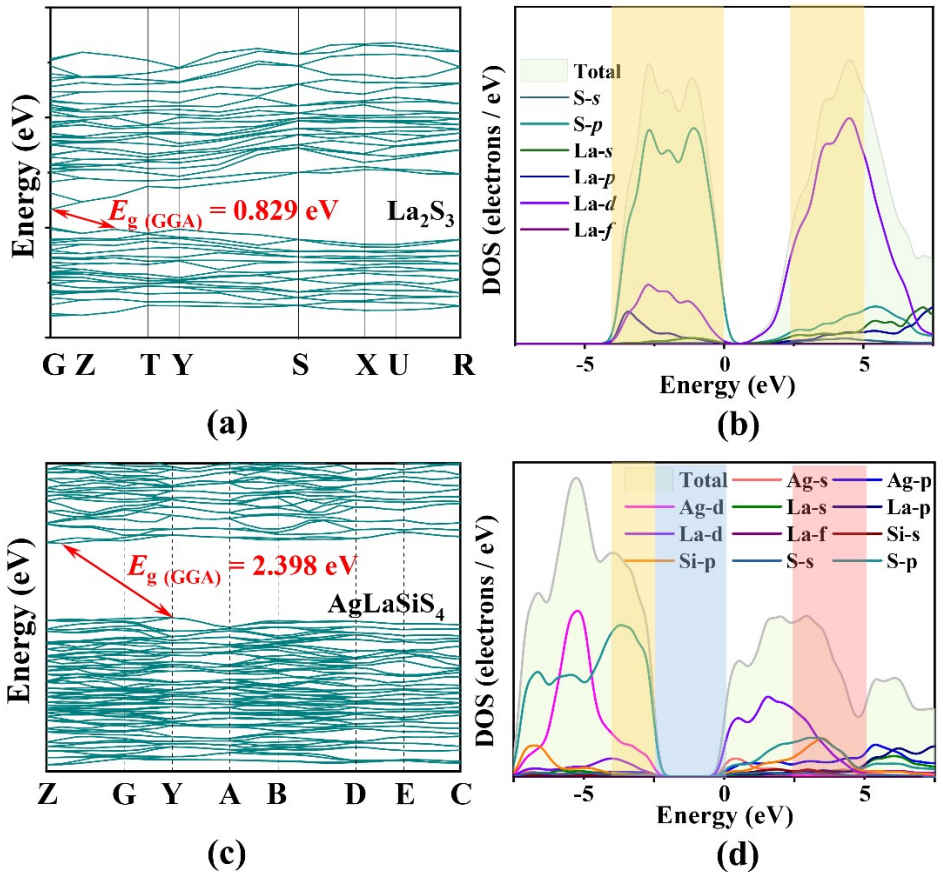

Figure S12. The band structures, and the total and partial density of states of La_2S_3 (a-b), $AgLaSiS_4$ (c-d).

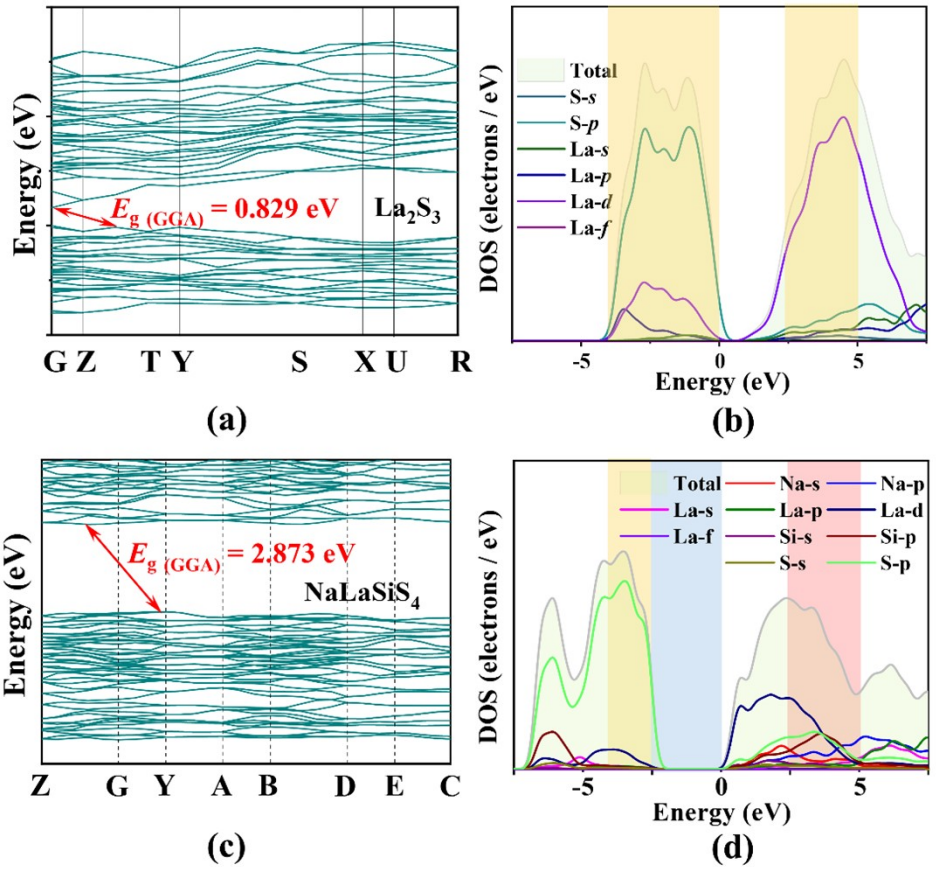

Figure S13. The band structures, and the total and partial density of states of La_2S_3 (a-b), $NaLaSiS_4$ (c-d).

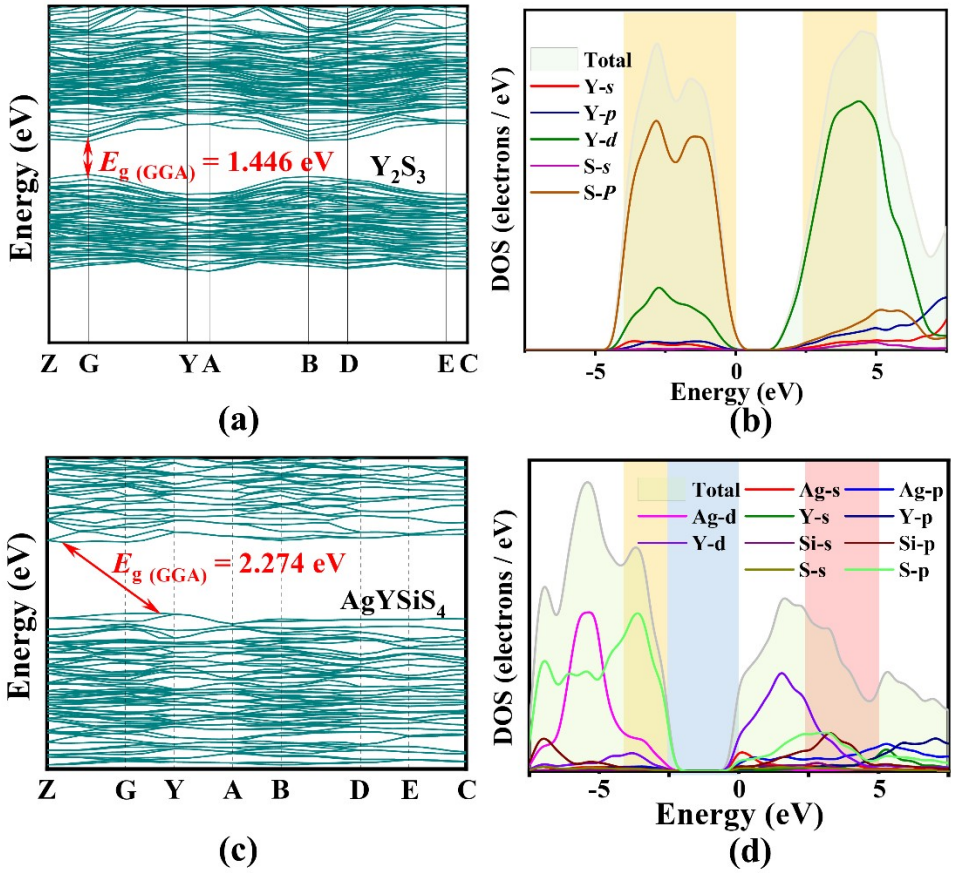

Figure S14. The band structures, and the total and partial density of states of Y_2S_3 (a-b), $AgYSiS_4$ (c-d).

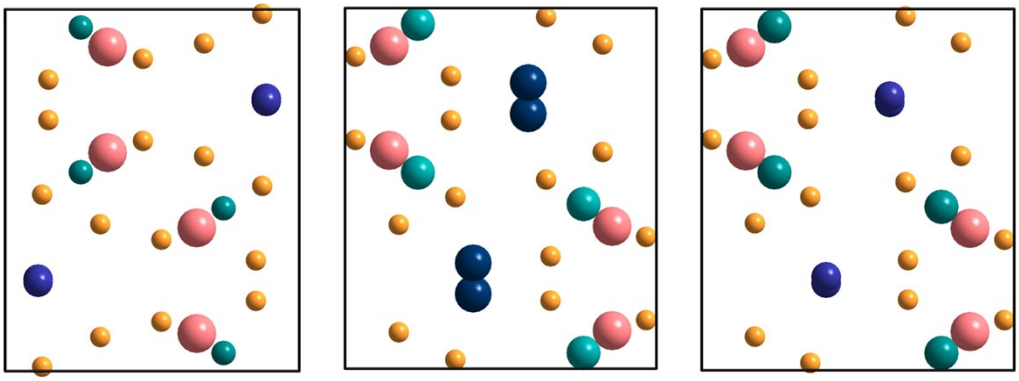

Figure S15. Atomic models of $AgLaSiS_4$ (a), $NaLaSiS_4$ (b) and the virtual $AgLaSiS_4$ (c) from $NaLaSiS_4$.

References

1. Y. Han, C. Hu, B. Li and J. Mao, $LnLiSiS_4$ (Ln = La and Ce): promising infrared nonlinear optical materials designed by aliovalent substitution from $SrCdSiS_4$, *Mater. Today Phys.*, 2023, **31**, 100987.
2. L. Dong, S. Zhang, P. Gong, L. Kang and Z. Lin, Evaluation and prospect of mid-infrared nonlinear optical materials in f^0 rare earth (RE = Sc, Y, La) chalcogenides, *Coord. Chem. Rev.*, 2024, **509**, 215805.
3. I. Hartenbach and T. Schleid, Thiosilicate der selten-erd-eemente: III. $KLa[SiS_4]$ und $RbLa[SiS_4]$ – ein struktureller vergleich, *Z. Anorg. Allg. Chem.*, 2005, **631**, 1365-1370.
4. G. Gauthier, F. Guillen, S. Jobic, P. Deniard, P. Macaudière, C. Fouassier and R. Brec, Synthesis, structure and electronic properties of the cerium and potassium thiosilicate: $KCeSiS_4$, *Comptes Rendus de l'Académie des Sciences - Series IIC - Chem.*, 1999, **2**, 611-616.
5. I. Hartenbach and T. Schleid, Thiosilicate der selten-erd-elemente: i. die isotypen verbindungen $KCe[SiS_4]$ und $Eu_2[SiS_4]$, *Z. Anorg. Allg. Chem.*, 2002, **628**, 1327-1331.
6. M. Usman, M. D. Smith, G. Morrison, V. V. Klepov, W. Zhang, P. S. Halasyamani and H. zur Loye, Molten alkali halide flux growth of an extensive family of noncentrosymmetric rare earth sulfides: structure and magnetic and optical (SHG) properties, *Inorg. Chem.*, 2019, **58**, 8541-8550.
7. Evenson and P. K. Dorhout, Synthesis and characterization of four new europium group XIV chalcogenides: K_2EuTSe_5 and $KEuTS_4$ (T = Si, Ge), *Inorg. Chem.*, 2001, **40**, 2409-2414.
8. A. Gray, J. Knaust, B. Chan, L. Polyakova and P. Dorhout, Crystal structure of potassium ytterbium (III) tetrathiosilicate, $KYbSiS_4$, *Z. Kristallogr. New cryst. struct.*, 2005, **220**, 313-313.
9. A. Choudhury, L. A. Polyakova, I. Hartenbach, T. Schleid and P. K. Dorhout, Synthesis, structures, and properties of layered quaternary chalcogenides of the general formula $ALnEQ_4$ (A= K, Rb; Ln= Ce, Pr, Eu; E= Si, Ge; Q= S, Se), *Z.*

Anorg. Allg. Chem., 2006, **632**, 2395-2401.

10. Y. Liu, X. Li, S. Wu, M. Ma, X. Jiang, Y. Wu and D. Mei, A rare earth chalcogenide nonlinear optical crystal $KLaGeS_4$: achieving good balance among band gap, second harmonic generation effect, and birefringence, *Inorg. Chem.*, 2024, **63**, 10938-10942.
11. D. Mei, W. Cao, N. Wang, X. Jiang, J. Zhao, W. Wang, J. Dang, S. Zhang, Y. Wu, P. Rao and Z. Lin, Breaking through the "3.0 eV wall" of energy band gap in mid-infrared nonlinear optical rare earth chalcogenides by charge-transfer engineering, *Mater. Horiz.*, 2021, **8**, 2330-2334.
12. P. Wu and J. A. Ibers, Synthesis and structures of the quaternary chalcogenides of the type $KLnMQ_4$ (Ln = La, Nd, Gd, Y; M = Si, Ge; Q = S, Se), *J. Solid State Chem.*, 1993, **107**, 347-355.
13. B. Chan and P. Dorhout, Crystal structures of potassium terbium (III) tetrasulfidogermanate, $KTbGeS_4$, and potassium praseodymium (III) tetraselenidogermanate, $KPrGeSe_4$, *Z. Kristallogr. New cryst. struct.* , 2005, **220**, 7-8.
14. B. R. Martin and P. K. Dorhout, Molten flux synthesis of an analogous series of layered alkali samarium selenogermanate compounds, *Inorg. Chem.*, 2004, **43**, 385-391.
15. A. Choudhury, L. A. Polyakova, I. Hartenbach, T. Schleid and P. K. J. I. c. Dorhout, Synthesis, structures, and properties of layered quaternary chalcogenides of the general formula $ALnEQ_4$ (A= K, Rb; Ln= Ce, Pr, Eu; E= Si, Ge; Q= S, Se), *Z. Anorg. Allg. Chem.*, 2006, **632**, 2395-2401.
16. I. Hartenbach and T. Schleid, The non-isotypic pair $CsCe[SiS_4]$ and $CsCe[SiSe_4]$: A structural comparison, *J. Alloy Compd.*, 2006, **418**, 95-100.
17. I. Hartenbach and T. Schleid, Thiosilicate der selten-erd-elemente: II. die nichtzentrosymmetrischen caesium-derivate $CsM[SiS_4]$ (M = Sm - Tm), *Z. Anorg. Allg. Chem.*, 2003, **629**, 394-398.
18. C. K. Bucher and S.-J. Hwu, $CsSmGeS_4$: a novel layered mixed-metal sulfide crystallizing in the noncentrosymmetric space group $P2_12_12_1$, *Inorg. Chem.*, 1994,

33, 5831-5835.